The Actual Incision Determines the Efficiency of Repair of Cisplatin-Damaged DNA by the *Escherichia coli* UvrABC Endonuclease†

R. Visse,* A. J. van Gool, G. F. Moolenaar, M. de Ruijter, and P. van de Putte

Laboratory of Molecular Genetics, Department of Biochemistry, Gorlaeus Laboratories, Leiden University, P.O. Box 9502, 2300 RA Leiden, The Netherlands

Received October 13, 1993; Revised Manuscript Received December 6, 1993®

ABSTRACT: The UvrABC endonuclease from *Escherichia coli* repairs a broad spectrum of DNA lesions with variable efficiencies. The effectiveness of repair is influenced by the nature of the lesion, the local DNA sequence, and/or the topology of the DNA. To get a better understanding of the aspects of this multistep repair reaction that determine the effectiveness of repair, we compared the incision efficiencies of linear DNA fragments containing either a site-specific *cis*-[$Pt(NH_3)_2$[d(GpG)-N7(1),-N7(2)}] or a *cis*-[$Pt(NH_3)_2$[d(GpCpG)-N7(1),-N7(3)}] adduct. Overall the DNA with the *cis*-PtGG adduct was incised about 3.5 times more efficiently than the *cis*-Pt.GCG-containing DNA. The rate of UvrB–DNA preincision complex formation for both lesions was similar and high in relation to the incision. DNase I footprints, however, showed that the local structure of the two preincision complexes is different. An assay was developed to measure the binding of UvrC to the preincision complexes and it was found that the binding rate of UvrC to the more slowly incised *cis*-Pt.GCG preincision complex was higher than to the *cis*-Pt.GG preincision complex. This most likely reflects a qualitative difference in preincision complex structures. For both lesions the binding of UvrC to the preincision complex was fast compared to the kinetics of actual incision. Apparently, direct incision of cisplatin damage requires an additional conformational change after the binding of UvrC.

The UvrABC endonuclease from *Escherichia coli* repairs damaged DNA by removing an oligonucleotide containing the damage [for reviews, see Van Houten (1990) and Lin and Sancar (1992a)]. The proteins that are involved in incision of the damaged DNA are UvrA (104 kDa), UvrB (76 kDa), and UvrC (68 kDa). The reaction proceeds in a sequential fashion in which formation of different macromolecular complexes culminates in highly specific incision of damaged DNA. The following stages in the repair process can be recognized. In solution UvrA forms a dimer, and although this complex is capable of damage recognition, the active complex *in vivo* most likely is a UvrB monomer bound to a UvrA dimer (Orren & Sancar, 1989). Upon binding of $UvrA_2B$ to the damaged site, the nucleoprotein complex changes conformation, which finally results in the so-called preincision complex. This complex is extremely stable with a half-life of 55 min (Yeung et al., 1986). It was found that the preincision complex contains only UvrB (Orren & Sancar, 1989, 1990; Visse et al., 1992) which was surprising as UvrB alone has no affinity for (damaged) DNA. Apparently conformational changes in the $UvrA_2B$–DNA complex allow UvrB binding. The release of UvrA from the complex enables it to act catalytically in the loading of UvrB (Orren & Sancar, 1990; Sancar & Hearst, 1993). Binding of UvrC to the preincision complex is essential for incision to take place. Although it is generally believed that UvrC binds to the complex after the release of UvrA, we have shown that preincision complexes still containing UvrA are also incision-proficient (Visse et al., 1992). The DNA is incised asymmetrically on both sides of the lesion, first the 3′ incision 4–5 phosphodiester bonds downstream of the lesion by UvrB in the UvrBC–DNA complex (Lin et al., 1992), followed by 5′ incision eight phosphodiester bonds upstream of the damaged site by UvrC (Lin & Sancar, 1992b). When UvrA remains in the preincision complex, this can lead to an additional incision at the 15th phosphodiester bond 5′ of the lesion (Visse et al., 1992). The remaining complex, the postincision complex, is stable and needs additional factors for turnover (Caron et al., 1985; Husain et al., 1985). The 12–13-mer oligonucleotide containing the damage and UvrC are released by UvrD (helicase II). DNA polymerase I then restores the integrity of the DNA by filling in the gap and detaching UvrB, and the remaining nick is sealed by ligase (Orren et al., 1992).

The UvrABC endonuclease reaction is relatively complex as opposed to a simple recognize-and-repair strategy observed for other repair proteins such as DNA glycosylases or photolyase [for a review, see Sancar and Sancar (1988)]. The basis for this complexity is most likely the versatility of the UvrABC DNA repair system which is capable of recognizing and processing structurally very different DNA lesions. Probably not the actual lesion in the DNA is recognized, however, but the perturbed DNA structure resulting from the lesion. The damage recognition process and the structural deformation of the DNA that is both necessary and sufficient to initiate repair are still not comprehended. Substrates for the endonuclease range from adducts that severely disturb the normal B-DNA structure, like HMT[1] (Sancar et al., 1985), *N*-AAAF (Seeberg & Fuchs, 1990), and cisplatin damage (Beck et al., 1985), to lesions that hardly affect the DNA structure, such as Ap sites (Lin & Sancar, 1989). Even

† This work was supported by the J. A. Cohen Institute for Radiopathology and Radiation Protection (I.R.S.).

* Corresponding author.

® Abstract published in *Advance ACS Abstracts,* February 1, 1994.

[1] Abbreviations: *cis*-Pt.GG, *cis*-[$Pt(NH_3)_2$[d(GpG)-N7(1),-N7(2)}]; *cis*-Pt.GCG, *cis*-[$Pt(NH_3)_2$[d(GpCpG)-N7(1),-N7(3)}]; cisplatin, *cis*-diamminedichloroplatinum(II); $PtCl_2$(en), dichloroethylenediamineplatinum(II); $PtCl_2$(dach), diamminecyclohexanedichloroplatinum(II); HMT, 4′-(hydroxymethyl)-4,5′,8-trimethylpsoralen; *N*-AAAF, *N*-acetoxy-*N*-(2-acetyl)aminofluorene.

0006-2960/94/0433-1804$04.50/0

noncovalent DNA binding drugs can be recognized and in some cases repaired (Selby & Sancar, 1991).

An important aspect of the UvrABC-dependent repair of DNA damage is further that not all lesions are repaired equally efficiently. Due to the complexity of the DNA excision repair process the overall efficiency is not only the result of the effectiveness of damage recognition but also of the individual processing steps. Therefore, in order to gain more insight in the repairability of the different damages it is important to analyze each individual step in the reaction.

In this study we have analyzed in detail the UvrABC-dependent incision of DNA containing a *cis*-Pt.GG or a *cis*-Pt.GCG lesion. Both adducts are intrastrand cross-links resulting from the reaction of the cytostatic agent cisplatin with the N7 positions of the guanines [for reviews, see Reedijk (1987) and Sherman and Lippard (1987)]. Although both DNA adducts are chemically identical, the conformational distortions of the DNA resulting from the two lesions are different. The *cis*-Pt.GG adduct introduces a kink and unwinds the DNA, but all the bases seem to be paired (Kozelka et al., 1987; Rice et al., 1988; Bellon et al., 1991). The *cis*-Pt.GCG adduct also unwinds the DNA but induces a site-directed bend in the DNA in which the base flanked by the platinated guanines seems to be unpaired and extrahelical (Mazeau et al., 1989; Anin & Leng, 1990; Bellon et al., 1991).

Results presented here show that for both cisplatin adducts the UvrC binding to the preincision complex and the actual incision can be studied as separate events. The efficiency of incision following UvrC binding to the preincision complex was different for the two cisplatin adducts. Implications for the mechanism of excision repair in *E. coli* with respect to damage recognition and processing are discussed.

MATERIALS AND METHODS

Isolation and Characterization of an Oligonucleotide Containing a Specific cis-Pt.GCG Adduct. Preparation of the 18-mer oligonucleotide with a specific *cis*-Pt.GCG adduct was essentially the same as the method used to isolate DNA with a *cis*-Pt.GG adduct (Visse et al., 1991). The oligonucleotide (5′ dAATTCCCACCGCGAACCA) was first purified by FPLC on a MonoQ column (Pharmacia LKB Biotechnology Inc., Uppsala, Sweden) with a NaCl gradient. The eluate was desalted by binding the oligonucleotide to a C-18 (Serva, New York) followed by elution with 25% acetonitrile; the eluate was dried down in a vacuum centrifuge. The oligonucleotide, 44 μg at a concentration of 80 μg/mL in H_2O, was treated with a 3-fold molar excess of *cis*-$Pt(NH_3)_2Cl_2$ at 37 °C. Aliquots were taken at regular intervals and reaction products were separated from free oligonucleotide by FPLC MonoQ. The samples were loaded at neutral pH in H_2O and eluted with a NaCl gradient at a flow rate of 1 mL/min. After sufficient progress of the reaction, platinated oligonucleotide was isolated using the same procedure. The NaCl was removed with C-18 and an aliquot was analyzed by FPLC MonoQ to check the purity. The presence and identity of the Pt adduct was confirmed by several different methods (results not shown): (i) The platinated oligonucleotide migrated as a single band on a 20% acrylamide/8 M urea gel and had a lower mobility than the control, unplatinated oligonucleotide. The normal mobility was restored by incubation with NaCN, which is known to remove platinum adducts from DNA (Comess et al., 1990). (ii) Restriction by *Thal* that recognizes the sequence CGCG in double-stranded DNA was inhibited by the platinum adduct. (iii) The association of the cisplatin adduct with the N7 position of the two guanines was checked by Maxam & Gilbert (1980) sequencing. The platinum adduct protects the base from the cleavage reaction (Comess et al., 1990; Visse et al., 1991). (iv) The nature of the platinum adduct (*cis*-[$Pt(NH_3)_2$-{d(GpCpG)-N7(1),-N7(3)}]) was confirmed using a quantitative immunochemical method (Fichtinger-Schepman et al., 1985, 1987). The platinated oligonucleotide was enzymatically degraded to unmodified mononucleotides and platinum-containing (di)nucleotides (Fichtinger-Schepman et al., 1985). The reaction products were separated on a MonoQ column and the presence of specific platinum adducts was determined and quantified in a competitive enzyme-linked immunoabsorbent assay (Fichtinger-Schepman et al., 1987). Only *cis*-$Pt(NH_3)_2d(GMP)_2$, the degradation product of *cis*-Pt.GCG, was detected.

Construction of a 96-bp Fragment with a Site-Specific Cisplatin Adduct. A 96-bp double-stranded DNA fragment with a specific *cis*-Pt.GG or *cis*-Pt.GCG adduct was constructed from the platinated 18-mer and five oligonucleotides using conditions as described before (Visse et al., 1991).

UvrABC Endonuclease Incision Assay. The subunits of the UvrABC endonuclease, UvrA, UvrB, and UvrC, were isolated as described before (Visse et al., 1992). The incision assays were performed in 50 mM Tris-HCl, pH 7.5, 10 mM $MgCl_2$, 1 mM ATP, 1 mM DTT, and 0.1 mg/mL BSA with 10 nM UvrA and 100 nM UvrB. After a 5-min incubation at 37 °C, 10 000 cpm (Cerenkov) of ^{32}P-labeled DNA and 10 or 37.5 nM UvrC were added and the incubation was continued at 37 °C. In the experiments where UvrA and UvrB were preincubated with the DNA, UvrC was added 20 min later. At distinct times after the addition of UvrC the reaction was stopped with 11 μL of 0.6 M sodium acetate, 77 mM EDTA, and 2 μg/mL calf thymus DNA. The DNA was isolated by phenol extraction, ethanol-precipitated, and analyzed on a 8% denaturing polyacrylamide gel. Kodak X-Omat AR5 film was used for autoradiography. The extent of incision was quantified by determining the amount of radioactivity (Cerenkov) in the gel slices.

UvrB–DNA Preincision Complex Formation. For the preincision complex formation the same conditions were used as with the incision assay: 10 nM UvrA and 100 nM UvrB were preincubated for 5 min at 37 °C, 25 000 cpm (Cerenkov) of ^{32}P-labeled DNA was added together with 62.5 ng of pBR322 as carrier DNA. The addition of carrier DNA did not affect the incision of the platinated DNA. After distinct times $CaCl_2$ was added to 2.5 mM together with 0.21 unit of DNase I (Pharmacia LKB Biotechnology Inc., Uppsala, Sweden). After exactly 1 min the incubation was stopped and analyzed as described above. An incubation without UvrA but with UvrA storage buffer was included as a control. The change in intensity of bands indicated was quantified by scanning the autoradiograms with a 2222-020 Ultrascan XL laser densitometer (Pharmacia LKB Biotechnology Inc., Uppsala, Sweden).

UvrC Binding Analysis. To measure the binding of UvrC to the preincision complex, UvrC antiserum was used. Incubation conditions were identical to those for an incision assay. UvrA (10 nM) and UvrB (100 nM) were preincubated for 5 min at 37 °C, then 10 nM UvrC was added together with about 10 000 cpm of platinated DNA. When UvrA and UvrB were preincubated with the DNA, UvrC was added after 20 min. Samples (10 μL) were taken from the reaction mixture and added to 1 μL of UvrC antiserum on ice. The antibody-bound complexes were separated from the unbound complexes by gel electrophoresis (Visse et al., 1992). The amount of

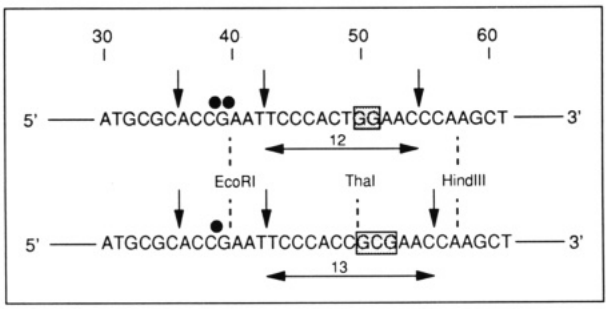

FIGURE 1: Sequence of the substrates with cisplatin adducts. Part of the sequence of the 96-bp DNA fragment containing either the *cis*-Pt.GG (above) or the *cis*-Pt.GCG adduct (below). The cisplatin is attached to the N7 of the guanines at positions 50 and 51 for the *cis*-Pt.GG or positions 50 and 52 for the *cis*-Pt.GCG adduct. UvrABC endonuclease incision positions are indicated by arrows. (●) DNase I-sensitive sites in the UvrB–DNA preincision complex. Relevant restriction sites are indicated. *Hpa*II cuts at position 64 (not shown).

complex bound by the antiserum was determined with a Betascope 603 blot analyzer (Betagen Corp.).

RESULTS

UvrABC Incision Sites on cis-Pt.GG- and cis-Pt.GCG-Containing DNA. For the comparison of the UvrABC repair efficiencies of *cis*-Pt.GG and *cis*-Pt.GCG DNA adducts, synthetic linear DNA fragments were used containing one specific adduct at a defined position (Figure 1). The 96-bp fragment was constructed from six individual oligonucleotides of which one contains the specific cisplatin adduct (Visse et al., 1991). Isolation and characterization of the 18-mer oligonucleotide with a specific *cis*-Pt.GCG adduct prior to the construction of the 96-bp fragment is described in Materials and Methods and was done as reported previously for the specific *cis*-Pt.GG adduct (Visse et al., 1991).

For the *cis*-Pt.GG adduct, UvrABC incision positions relative to the lesion have been analyzed before (Visse et al., 1991). The 5′ incision is at position 42; this is eight phosphodiester bonds upstream of guanine 50. An additional 5′ incision is observed at position 39, 15 phosphodiester bonds from the lesion. We have shown before (Visse et al., 1991, 1992) that the additional 5′ incision is due to preincision complexes still containing UvrA.

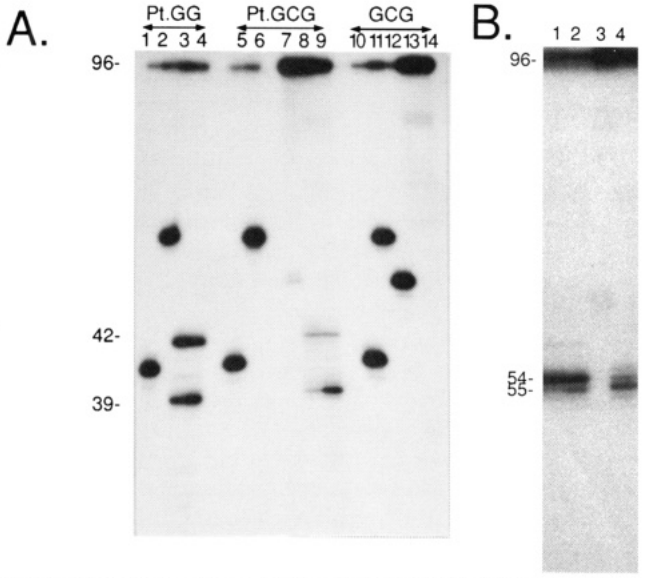

FIGURE 2: UvrABC incision of DNA with *cis*-Pt.GG or *cis*-Pt.GCG adduct. (A) 5′ ^{32}P-labeled 96-bp fragment with a *cis*-Pt.GG (lanes 1–4) or a *cis*-Pt.GCG adduct (lanes 5–9) and unplatinated DNA with the GCG sequence as a control (lanes 10–14) were incubated with 10 nM UvrA, 100 nM UvrB, and 10 (lanes 3, 8, and 13) or 37.5 nM UvrC (lanes 4, 9, and 14) using conditions as described in Materials and Methods. The 5′ incision at position 42 and the additional incision at position 39 are indicated. The presence of the *cis*-Pt.GCG adduct in the 96-bp fragment inhibits *Tha*I digestion, which recognizes the sequence CGCG (compare lanes 7 and 12). Digestions with *Eco*RI (lanes 1, 5, and 10) and *Hin*dIII (lanes 2, 6, and 11), the recognition sites of which do not contain platinated nucleotides, are not affected. (B) The incision positions downstream of the cisplatin adduct were determined with DNA fragments that were ^{32}P-labeled 3′ in the damaged strand. *cis*-Pt.GG (lanes 1–3) or *cis*-Pt.GCG (lane 4) containing DNA was incubated with 20 nM UvrA, 100 nM UvrB, and 10 nM UvrC (lanes 1 and 4) or 40 nM UvrA, 100 nM UvrB, and 10 nM UvrC (lane 2) or 20 nM UvrA and 100 nM UvrB (lane 3) as described in Materials and Methods. The positions of incision have been determined before for *cis*-Pt.GG (Visse et al., 1991).

We compared the positions of UvrABC-induced incisions for the *cis*-Pt.GG and *cis*-Pt.GCG lesions (Figure 2). The 5′ incisions of DNA containing the *cis*-Pt.GCG or *cis*-Pt.GG adduct are found at identical positions (Figure 2A, positions 42 and 39, compare lanes 8/9 with 3/4). The 3′ incision of both lesions is less well defined as different bands are present

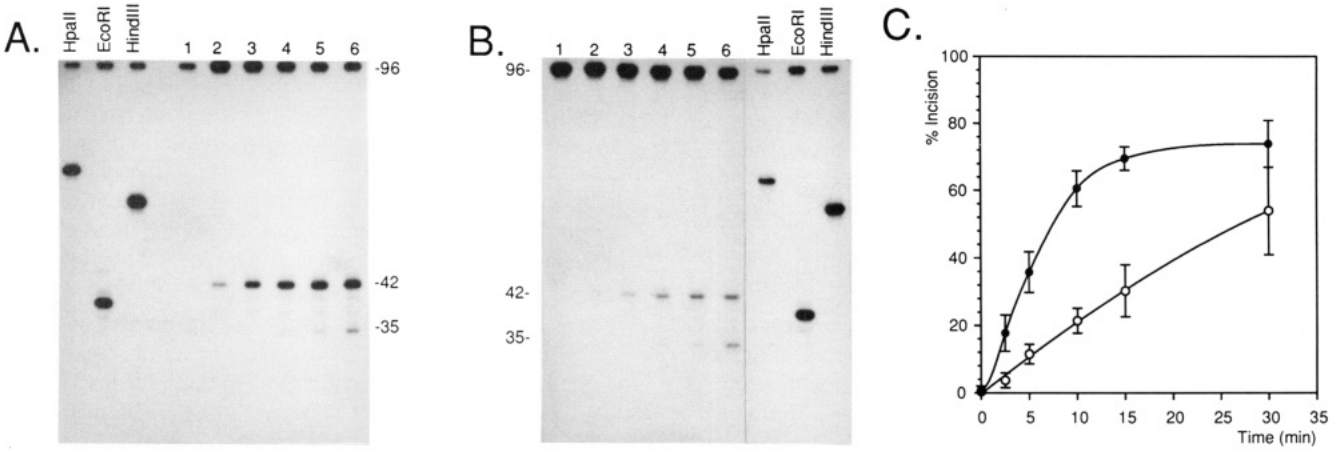

FIGURE 3: Rate of UvrABC incision of *cis*-Pt.GG- and *cis*-Pt.GCG-containing linear DNA. 5′ ^{32}P-labeled DNA containing either (A) *cis*-Pt.GG or (B) *cis*-Pt.GCG were incubated with 10 nM UvrA, 100 nM UvrB, and 10 nM UvrC for 0, 2.5, 5, 10, 15, or 30 min (lanes 1–6, respectively) using conditions described in Materials and Methods. Digestions with *Hpa*II were done to determine the amount of double-stranded DNA. *Eco*RI and *Hin*dIII digestions were incorporated as size markers. Each band was cut from the gel to quantify the amount of radioactivity (Cerenkov radiation). (C) Graphic presentation of the time-dependent incision of *cis*-Pt.GG- (●) and *cis*-Pt.GCG- (○) containing DNA. The data are the average of four (GG) or five (GCG) independent experiments. The amount of incision is expressed as the percentage of incision with respect to the level of *Hpa*II digestion of the same fragment.

(Figure 2B, lanes 1, 2, and 4). The position of the major 3′ incision is clearly different for the two lesions, position 54 for *cis*-Pt.GG and 55 for *cis*-Pt.GCG (Figure 2B, lanes 1, 2, and 4). The distance with respect to the 3′ damaged guanine, however, is the same in both cases, four phosphodiester bonds. The majority of the excised fragments therefore will be 13 nucleotides in length for *cis*-Pt.GCG and 12 for *cis*-Pt.GG.

UvrABC Incision of DNA with a cis-Pt.GG Adduct Is More Efficient Than DNA with a cis-Pt.GCG Lesion. The kinetics of overall incision on DNA with the *cis*-Pt.GG adduct was compared to that of *cis*-Pt.GCG-containing DNA. DNA fragments ^{32}P-labeled 5′ in the damaged strand were incubated with concentrations of the UvrABC subunits that are within the range they are found *in vivo* (Sancar & Sancar, 1988), 10 nM UvrA, 100 nM UvrB, and 10 nM UvrC. In these experiments the amount of protein was always in excess with respect to that of the DNA. At distinct times the reaction was stopped and the DNA was isolated and analyzed on a denaturing gel to visualize incision (Figure 3A,B). The level of *Hpa*II digestion of a particular substrate preparation was used to define the maximum available double-stranded substrate. *Hpa*II only cuts double-stranded DNA and therefore allows us to correct for the presence of single-stranded DNA in our substrate preparations, which is not repaired by UvrABC. The percentage of UvrABC incision was calculated relative to the level of *Hpa*II digestion. The time course of UvrABC incision of DNA with *cis*-Pt.GG or *cis*-Pt.GCG is presented in Figure 3C and summarizes the data of at least four independent experiments. Results show that incision of DNA with the *cis*-Pt.GG adduct is more efficient than with the *cis*-Pt.GCG adduct. The initial rate of incision for the *cis*-Pt.GG adduct was 7.1% min^{-1} and for the *cis*-Pt.GCG-containing DNA 2.1% min^{-1}, a difference of about a factor of 3.4. Since at 30 min the incision of *cis*-Pt.GCG not yet reached its plateau value, we cannot see whether the maximum level of this lesion is different from that of *cis*-Pt.GG.

Preincision Complex Formation on cis-Pt.GG and cis-Pt.GCG. We have determined which step of the UvrABC incision reaction is responsible for the difference in incision efficiencies observed for the two cisplatin lesions. First we compared the DNase I footprint patterns of the preincision complexes on the two lesions. Both show a protected region of 19–20 bp, which is comparable to that found for other lesions. Indicative for the formation of a preincision complex is the occurrence of DNase I-sensitive site(s) upstream of the 5′ incision site as a result of a conformational change in the DNA (Van Houten et al., 1987; Seeberg & Fuchs, 1990; Snowden & Van Houten, 1991; Visse et al., 1991). Also, preincision complexes formed on both cisplatin–DNA adducts give rise to such an enhanced DNAseI sensitivity (Figure 4). The *cis*-Pt.GG results in two of these enhanced cleavage sites (positions 38 and 39) whereas the *cis*-Pt.GCG DNA only shows one (position 38), despite the fact that the sequence in this region is the same (Figure 1). As DNase I activity is dependent on the DNA conformation [reviewed by Travers (1989)], this shows that the structure of the DNA in the preincision complexes formed on *cis*-Pt.GG and *cis*-Pt.GCG must be locally different.

To determine the rate of preincision complex formation on both lesions, UvrA and UvrB were incubated with the DNA substrate for 0, 2, 5, 10, and 20 min followed by a DNase I incubation for 1 min. Subsequently the DNA was isolated and analyzed on a denaturing polyacrylamide gel (Figure 4A). As an indicator for preincision complex formation we used the DNase I sensitivity of position 38. To determine the rate

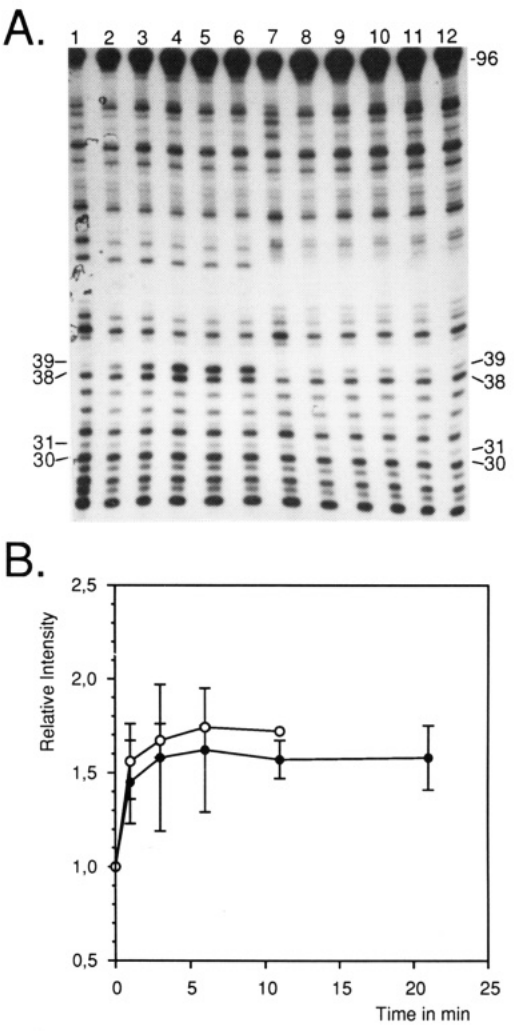

FIGURE 4: Preincision complex formation by $UvrA_2B$. (A) The 5′ labeled DNA fragments were incubated with 10 nM UvrA and 100 nM UvrB for 0, 2, 5, 10, and 20 min; this was followed by a 1-min DNase I treatment, bringing the total incubation time to 1, 3, 6, 11, and 21 min, respectively (lanes 1–6 and 7–12 for *cis*-Pt.GG- and *cis*-Pt.GCG-containing DNA, respectively). The 0-min incubation (lanes 1 and 7) was obtained by leaving out UvrA to prevent protein binding during the 1-min DNase I incubation. The intensities of the indicated bands were quantified by laser densitometry. The bands at positions 30 and 31, outside the area of the protein binding, are internal controls. (B) First, for each lane the ratio of the intensities of the DNase I-sensitive site (positions 38) to the controls (positions 30 and 31 combined) was determined. These values of each time point are plotted relative to that of $t = 0$. The data represent the average of two (*cis*-Pt.GCG, ○) or three (*cis*-Pt.GG, ●) independent experiments.

of preincision complex formation we measured the kinetics of appearance of band 38. As an internal control to correct for variations in the amount of radioactivity loaded on the gel or variability in DNase I degradation we also measured the intensity of two other bands located outside the footprint (30 and 31). The results represented in Figure 4B illustrate that the rate of formation of the DNase I-sensitivity site at position 38 appears to be the same for both adducts and reaches a maximum already after about 3 min. Apparently the formation of the preincision complex on both lesions is much faster than the incision of the platinated DNA (compare Figures 4B and 3C), implying that the preincision complex formation is not the rate-determining factor of the incision process. This was confirmed in experiments in which prior to UvrC addition UvrA and UvrB were preincubated with the DNA. If preincision complex formation would be slow, then preincubation is expected to increase the incision rate.

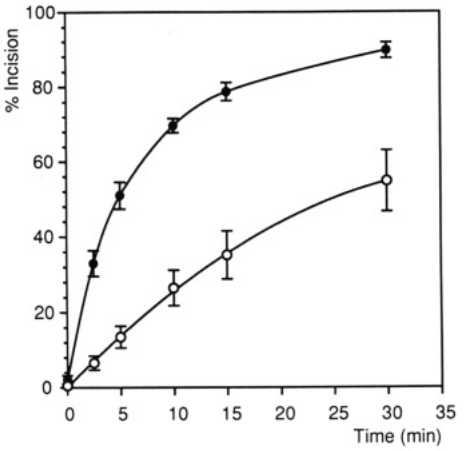

FIGURE 5: Rate of incision of the platinated DNA after preincubation with UvrA and UvrB. The experimental conditions are the same as described in Figure 3 except that UvrA and UvrB were preincubated with the platinated DNA fragments for 20 min. The reaction was stopped at 0, 2.5, 10, 15, or 30 min after the subsequent addition of UvrC. The percentage of incision was determined and plotted. The data represent the average of three independent experiments. (●) *cis*-Pt.GG- and (○) *cis*-Pt.GCG-containing DNA, respectively.

However, the time-dependent incision observed after preincubation (Figure 5) is similar to the incision curve without preincubation (compare with Figure 3C). Thus the difference in incision efficiencies of the two lesions is determined by a reaction step beyond that of preincision complex formation.

The Actual Incision Event and Not the UvrC Binding Is Rate Limiting. The next step in the processing of damaged DNA is the binding of UvrC to the preincision complex. The difference in incision efficiencies observed for the two lesions could be due to differential recognition of the preincision complexes by UvrC. On the other hand, the difference could also be related to unequal efficiencies of the actual incision in the two UvrBC-damaged DNA complexes.

To distinguish between both possibilities we developed a method to measure the time-dependent binding of UvrC to the preincision complex. Complexes bound by UvrC can be separated from unbound preincision complexes with UvrC antiserum in a gel mobility shift assay (Visse et al., 1992). The amount of radioactivity retarded by the UvrC antibodies is a measure for the UvrC binding to the preincision complex.

Before measuring the kinetics of UvrC binding we first demonstrated the specificity of this assay (Figure 6A). The 5′-labeled 96-bp fragments were preincubated with UvrA and UvrB (10 and 100 nM, respectively) for 20 min. Aliquots of the reaction mixture were then incubated on ice with UvrB antiserum, UvrC preserum, or UvrC antiserum (Figure 6A, samples 1–3 respectively). Sample 1 shows that a substantial amount of UvrB is associated with the platinated DNA. Samples 2 and 3 demonstrate that the UvrC antiserum has some cross-reactivity with UvrB, which has been observed before (Visse et al., 1992). When UvrC (10 nM) was added to the mixture and aliquots were taken after 0, 1, and 2.5 min and incubated with UvrC antiserum on ice, a time-dependent increase in the amount of UvrC antiserum complexed radioactivity was observed. The percentage of complex measured at $t = 0$ after the addition of UvrC and UvrC antiserum is comparable to the UvrB cross-reactivity (compare samples 3 and 4). This shows that incubation with the UvrC antiserum instantly inhibits further binding of UvrC to the preincision complex. When UvrA is omitted from the incubation mixture no UvrC is bound (sample 7). On

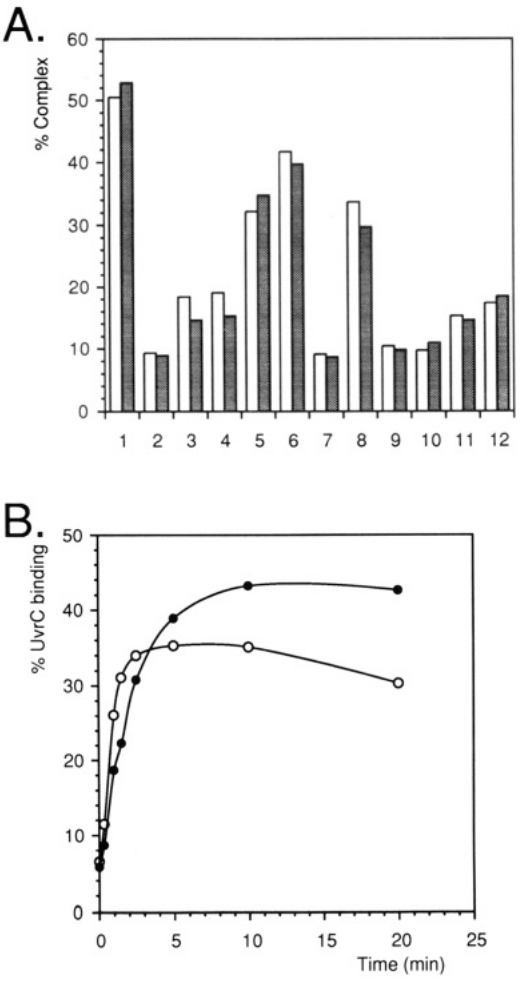

FIGURE 6: Rate of UvrC binding to the preincision complex. The binding of UvrC was measured using UvrC antiserum. The antibody-bound complexes were separated from unbound complexes by gel electrophoresis. The percentage of radioactivity in the complex was measured and plotted. (A) UvrA (10 nM) and UvrB (100 nM) were incubated using standard conditions for 20 min with GG (open bars) or GCG (hatched bars) containing DNA with (samples 1–7) or without (samples 8–12) a platinum adduct. Aliquots of the incubation mixture were added to UvrB antiserum (sample 1), UvrC preserum (sample 2), or UvrC antiserum (sample 3). UvrC (10 nM) was added and the reaction was stopped with UvrC antiserum after 0, 1, and 2.5 min (samples 4–6). For 0 min incubation the UvrAB incubation mixture was added to the UvrC antiserum which was immediately followed by the addition of UvrC. Almost no UvrC binding is observed without UvrA in the incubation mixture (sample 7). Aliquots of the incubation mixture containing UvrA, UvrB, and nonplatinated DNA were added to UvrB antiserum (sample 8) and UvrC preserum (sample 9). UvrC (10 nM) was added and the reaction was stopped with UvrC antiserum after 0, 1, and 2.5 min (samples 10–12). (B) The time-dependent UvrC binding to the preincision complex was determined by incubating the 5′ ^{32}P-labeled DNA fragments with 10 nM UvrA, 100 nM UvrB, and 10 nM UvrC at 37 °C using standard conditions. Samples were taken at the indicated times and the reaction was stopped by addition to UvrC antiserum on ice. The amount of UvrC binding was determined as described above. (●) *cis*-Pt.GG- and (○) *cis*-Pt.GCG-containing DNA, respectively.

unplatinated DNA incubated with UvrA and UvrB also a substantial amount of radioactivity is complexed with UvrB antiserum (sample 8). This is not surprising as $UvrA_2B$ has affinity for undamaged DNA. With such a complex only a limited amount of UvrC binding is observed, which is probably due to lesions that are always present in synthetic DNA (Yeung et al., 1988). In spite of this background, the results demonstrate that specific binding of UvrC to the platinum-containing preincision complexes can be determined.

With this assay we measured the time-dependent UvrC binding to preincision complexes formed on the 96-bp fragment containing either *cis*-Pt.GG or *cis*-Pt.GCG (Figure 6B). The fragments were incubated with UvrA, UvrB, and UvrC, and at the indicated times aliquots of the reaction mixture were taken and the reaction was stopped with UvrC antiserum. The amount of radioactivity retained by the antibody complex was measured as described above and is plotted in Figure 6B. For both lesions a maximum value is reached within 5 min of incubation. This shows that compared to incision (Figure 3C) the binding of UvrC is fast. The rate-limiting step in the UvrABC-dependent incision of cisplatin-damaged DNA seems therefore to be beyond UvrC binding. The results further show that the rate of UvrC binding to the slowly incised *cis*-Pt.GCG preincision complex is higher than to the *cis*-Pt.GG preincision complex. A higher binding rate of UvrC with the *cis*-Pt.GCG preincision complex was also observed when prior to UvrC addition the DNA was preincubated with UvrA and UvrB to allow formation of the UvrB–DNA preincision complex (results not shown). The difference in UvrC binding rate therefore is a characteristic of the two preincision complexes most likely reflecting conformational differences.

The observation that UvrC binds faster to the more slowly incised *cis*-Pt.GCG preincision complex means that the induction of the actual incision in the UvrBC–DNA complex is even more difficult for *cis*-Pt.GCG than the difference in incision efficiencies suggest. The rapid binding of UvrC to a preincision complex is not sufficient to provoke an immediate incision, suggesting that an additional conformational change is required before incision can occur.

DISCUSSION

The UvrABC endonuclease has the potential to repair a large variety of DNA damages. These lesions range from bulky DNA adducts to Ap sites (Lin & Sancar, 1989), and even lesions with noncovalent DNA binding chemicals can be repaired (Lambert et al., 1989; Selby & Sancar, 1991). Although the enzyme has the proficiency to repair structurally different DNA lesions, the efficiency of the reaction is subject to large variations. Besides the nature of the lesion also neighboring sequences and the DNA topology can contribute to differences in the overall repair. Comparison of the efficiency of UvrABC repair of the cisplatin adducts to that of other lesions described in literature is difficult as different DNA substrates, enzyme preparations, and incubation conditions were used. Nevertheless, it is clear that DNA with lesions like anthramycin–N2-guanine (Nazimiec et al., 1992), HMT monoadducts (Munn & Rupp, 1991), or benzo[*a*]pyrene adducts (Tang et al., 1992) is incised very effectively. Incision of the HMT monoadduct, for example, is almost complete within 2 min of incubation with UvrABC (Munn & Rupp, 1992). The repair of cisplatin–DNA adducts reported here is much slower and of the same order of magnitude as observed for a pyrimidine dimer on linear DNA (Nazimiec et al., 1992).

The nature of the UvrABC endonuclease reaction also complicates the comparison of repair efficiencies. It is a multistep process that achieves high specificity through a so-called "selectivity cascade" (Lin & Sancar, 1992a). The sequence of the reaction can be divided into several distinct events: (1) initial recognition of a lesion by $UvrA_2B$, (2) the formation of the preincision complex, and (3) UvrC binding which is followed by the 3′ and 5′ incision of the damaged strand. Detailed information on these individual steps in the reaction is, however, only available for a limited number of lesions.

The selective recognition of the cisplatin lesions, which is attributed to UvrA acting as a dimer or as part of the $UvrA_2B$ complex, seems not very high. This is based on earlier experiments where it was found to be difficult to distinguish damage specific $UvrA_2$ binding from nonspecific binding (Visse et al., 1991). In this respect cisplatin seems to behave like a pyrimidine dimer on a linear DNA fragment (Bertrand-Burggraf et al., 1991). In the work presented here we show that in our experimental setup, with a high ratio of damaged versus undamaged bases in the DNA fragment and high protein concentrations relative to the DNA, the damage recognition is not determining the rate of the repair reaction. However, the poor damage recognition will have an influence on the maximum level of incision that can be observed in the experiments. Although the selective affinity of UvrA for damaged DNA over nondamaged DNA is not very high to begin with (Van Houten et al., 1987), other DNA lesions such as the HMT monoadduct (Van Houten et al., 1987) and also the less perturbing Ap site (Snowdon & Van Houton, 1991) are efficiently recognized in an *in vitro* system. Here we show that the formation of the UvrB–DNA preincision complex on the cisplatin-damaged DNA fragments was fast, indicating that once the damage is recognized the first processing step is highly productive.

The formation of the UvrB–DNA preincision complexes on DNA with a *cis*-Pt.GG or a *cis*-Pt.GCG was of a comparable efficiency and not responsible for the observed slow incision rates of these lesions. This is clearly different from Ap or modified Ap sites where it was demonstrated that the formation of the UvrB–DNA preincision complex was rate-limiting (Snowden & Van Houten, 1991).

In this paper we have described a method to measure the binding of UvrC to the preincision complex. In this way we could measure separately the kinetics of the kinetics of the actual binding of UvrC and the UvrC-induced incision. The UvrC binding to the preincision complexes was found to be fast relative to the incision of the DNA. This demonstrates that the binding of UvrC to the preincision complex alone does not result in immediate incision and that most likely additional conformational changes in the UvrBC–DNA complex are required. Since we did not observe uncoupling of the 5′ and 3′ incision, these conformational changes seem necessary for the 3′ incision catalyzed by UvrB.

The maximum amount of complex detected in the UvrC binding assay is for both adducts lower than the total amount of incision observed (compare Figures 6B and 3C). The reason for this discrepancy probably lies in the difference of the methods used. Incision is observed as the irreversible accumulation of strand breaks, whereas measuring the amount of UvrC binding depends on the detection of a specific complex which may dissociate during the experimental procedure. This means that the binding assay is well suited to determine the UvrC binding rate but not to measure the absolute amount of UvrC binding. Furthermore, the results show that the plateau value of UvrC binding to *cis*-Pt.GCG-containing DNA is lower than for *cis*-Pt.GG. This is most likely a reflection of a difference in the amount or stability of the preincision complexes formed for both adducts.

The slow incision of cisplatin-damaged DNA implies that *in vivo* there is a high probability that unprocessed Uvr–DNA complexes are encountered by the DNA replication machinery. This could be related to the observation by Brouwer et al. (1981, 1988) that the mutation induction by cisplatin is UvrAB-dependent. The mechanism of this process, however, is still unresolved.

The *cis*-Pt.GG and *cis*-Pt.GCG adducts behave differently in several aspects of the reaction. Although the rate of preincision complex formation is the same for both adducts, the resulting complex is not. The *cis*-PtGCG preincision complex has one DNase I sensitive site and the *cis*-Pt.GG preincision complex has two such sites despite the identical local sequence of both substrates, indicating that there are differences in the DNA structure between these preincision complexes (more data to be published elsewhere). This shows that the structure of the preincision complex is not strictly defined but allows a certain degree of adaptation to the lesion to which it is bound. On one hand this versatility of the preincision complex most likely contributes to the ability to handle different lesions, but on the other hand it can affect the efficiencies of the following steps in the reaction since the binding of UvrC to the preincision complex is faster for *cis*-Pt.GCG than for *cis*-Pt.GG.

The cisplatin–DNA adducts are more slowly repaired in comparison to bulky monoadducts (Nazimiec et al., 1992; Tang et al., 1992; Munn & Rupp, 1991). An important factor in this could be that the cisplatin lesions are intrastrand cross-links that restrict the dynamics of the DNA, thereby making it more difficult for the Uvr proteins to induce local conformational changes.

As the two cisplatin–DNA adducts are chemically identical, the observed differences in processing of the *cis*-Pt.GG and *cis*-Pt.GCG lesions are probably related to the structure of the cisplatin–DNA complexes. One aspect could be that the *cis*-Pt.GCG lesion is larger, spanning a "longer" stretch of DNA than the *cis*-Pt.GG adduct. As a result a 13-mer oligonucleotide for *cis*-Pt.GCG and a 12-mer for *cis*-Pt.GG is removed. However, this cannot be the only factor determining the incision efficiency. This is illustrated by the findings of Page et al. (1990), who compared the overall UvrABC-dependent incision of DNA fragments with a specific $PtCl_2$(en) or a $PtCl_2$(dach) adduct. They found that a GNG lesion was repaired faster than a GG lesion. Apparently the structures of the GG and GNG lesions with $PtCl_2$(en) or $PtCl_2$(dach) differ from those of cisplatin in such a way that the order of repair efficiencies is reversed. However, it is not known to what level the local sequence contexts, which are different in both studies, contribute to the repair efficiencies. Only analysis of the individual steps of the UvrABC endonuclease action on the $PtCl_2$(en) and $PtCl_2$(dach) adducts in the same sequence context could reveal where the reaction differs from that of DNA with cisplatin adducts.

Besides cisplatin-induced lesions, there are also other lesions for which the incision step could be rate-limiting. Munn & Rupp (1991) showed that a preincision complex is readily formed on a HMT interstrand cross-link but that for the incision step negative supercoiling of the DNA is required. Although no discrimination between UvrC binding to the preincision complex and the actual incision was made, the work presented here shows that the formation of a preincision complex on a linear DNA substrate is sufficient to allow rapid UvrC binding. This suggests that in the case of the HMT interstrand cross-link it is probably the incision step itself which is facilitated by the superhelicity of the DNA. Other examples of lesions with different incision efficiencies due to a late event in the reaction have been found with *N*-AAAF adducts on the three guanines of a *Nar*I site (Seeberg & Fuchs, 1990). Analysis of the structures of the three different adducts has revealed that the most inefficiently repaired adduct is intercalated in the helix whereas the other two are not (Belguise-Valladier & Fuchs, 1991). Preincision complexes are readily formed on all three lesions but they differ in the level of incision, suggesting again that the local structure of the lesion is important for the actual incision.

The precise nature of the presumed changes in the nucleoprotein complex after UvrC binding has occurred that lead to incision are not known. The fast binding of UvrC followed by the slow incision of the *cis*-Pt.GCG adduct seem to make this substrate specifically suitable to study these changes.

ACKNOWLEDGMENT

We are indebted to Dr. A. M. J. Fichtinger-Schepman and W. C. M. van Dijk-Knijnenburg for confirming the presence of the specific *cis*-Pt.GCG adduct with a quantitative immunochemical method and to Dr. J. Reedijk for his gift of cisplatin. Dr. N. Goosen is acknowledged for critical reading of the manuscript.

REFERENCES

Anin, M.-F., & Leng, M. (1990) *Nucleic Acids Res. 18*, 4395–4400.

Beck, D. J., Popoff, S., Sancar, A., & Rupp, W. D. (1985) *Nucleic Acids Res. 13*, 7395–7413.

Belguise-Valladier, P., & Fuchs, R. P. P. (1991) *Biochemistry 30*, 10091–10100.

Bellon, S. F., Coleman, J. H., & Lippard, S. J. (1991) *Biochemistry 30*, 8026–8035.

Bertrand-Burggraf, E., Selby, C. P., Hearst, J. E., & Sancar, A. (1991) *J. Mol. Biol. 219*, 27–36.

Brouwer, J., van de Putte, P., Fichtinger-Schepman, A. M. J., & Reedijk, J. (1981) *Proc. Natl. Acad. Sci. U.S.A. 78*, 7010–7014.

Brouwer, J., Vollebrecht, L., & van de Putte, P. (1988) *Nucleic Acids Res. 16*, 7703–7711.

Caron, P. R., Kushner, S. R., & Grossman, L. (1985) *Proc. Natl. Acad. Sci. U.S.A. 82*, 4925–4929.

Comess, K. M., Costello, C. E., & Lippard, S. J. (1990) *Biochemistry 29*, 2102–2110.

Fichtinger-Schepman, A. M. J., Baan, R. A., Luiten-Schuite, A., van Dijk, M., & Lohman, P. H. M. (1985) *Chem.-Biol. Interact. 55*, 275–288.

Fichtinger-Schepman, A. M. J., van Oosterom, A. T., Lohman, P. H. M., & Berends, F. (1987) *Cancer Res. 47*, 3000–3004.

Husain, I., Van Houten, B., Thomas, D. C., Abdel-Monem, M., & Sancar, A. (1985) *Proc. Natl. Acad. Sci. U.S.A. 82*, 6774–6778.

Kozelka, J., Archer, S., Petsko, G. A., & Lippard, S. J. (1987) *Biopolymers 26*, 1245–1271.

Lambert, B., Jones, B. K., Roques, B. P., Le Pecq, J.-B., & Yeung, A. T. (1989) *Proc. Natl. Acad. Sci. U.S.A. 86*, 6557–6561.

Lin, J.-J., & Sancar, A. (1989) *Biochemistry 28*, 7979–7984.

Lin, J.-J., & Sancar, A. (1992a) *Mol. Microbiol. 6*, 2219–2224.

Lin, J.-J., & Sancar, A. (1992b) *J. Biol. Chem. 267*, 17688–17692.

Lin, J.-J., Phillips, A. M., Hearst, J. E., & Sancar, A. (1992) *J. Biol. Chem. 267*, 17693–17700.

Maxam, A. M., & Gilbert, W. (1980) *Methods Enzymol. 65*, 499–560.

Mazeau, K., Vovelle, F., Rahmouni, A., Leng, M., & Ptak, M. (1989) *Anti-Cancer Drug Des. 4*, 63–78.

Munn, M. M., & Rupp, W. D. (1991) *J. Biol. Chem. 266*, 24748–24756.

Nazimiec, M., Grossman, L., & Tang, M.-S. (1992) *J. Biol. Chem. 267*, 24716–24724.

Orren, D. K., & Sancar, A. (1989) *Proc. Natl. Acad. Sci. U.S.A. 86*, 5237–5241.

Orren, D. K., & Sancar, A. (1990) *J. Biol. Chem. 265*, 15796–15803.

Orren, D. K., Selby, C. P., Hearst, J. E., & Sancar, A. (1992) *J. Biol. Chem. 267*, 780–788.
Page, J. D., Husain, I., Sancar, A., & Chaney, S. G. (1990) *Biochemistry 29*, 1016–1024.
Reedijk, J. (1987) *Pure Appl. Chem. 59*, 181–192.
Rice, J. A., Crothers, D. M., Pinto, A. L., & Lippard, S. J. (1988) *Proc. Natl. Acad. Sci. U.S.A. 85*, 4158–4161.
Sancar, A., & Sancar, G. B. (1988) *Annu. Rev. Biochem. 57*, 29–67.
Sancar, A., & Hearst, J. E. (1993) *Science 259*, 1415–1420.
Sancar, A., Franklin, K. A., Sancar, G. B., & Tang, M. S. (1985) *J. Mol. Biol. 184*, 725–734.
Seeberg, E., & Fuchs, R. P. P. (1990) *Proc. Natl. Acad. Sci. U.S.A. 87*, 191–194.
Selby, C., & Sancar, A. (1991) *Biochemistry 30*, 3841–3849.
Sherman, S. E., & Lippard, S. J. (1987) *Chem. Rev. 87*, 1153–1181.
Snowden, A., & Van Houten, B. (1991) *J. Biol. Chem. 220*, 19–33.
Tang, M.-S., Pierce, J. R., Doisy, R. P., Nazimiec, M. E., & Macleod, M. C. (1992) *Biochemistry 31*, 8429–8436.
Travers, A. A. (1989) *Annu. Rev. Biochem. 58*, 427–452.
Van Houten, B. (1990) *Microbiol. Rev. 54*, 18–51.
Van Houten, B., Gamper, H., Sancar, A., & Hearst, J. E. (1987) *J. Biol. Chem. 262*, 13180–13187.
Visse, R., de Ruijter, M., Brouwer, J., Brandsma, J. A., & van de Putte, P. (1991) *J. Biol. Chem. 266*, 7609–7617.
Visse, R., de Ruijter, M., Moolenaar, G. F., & van de Putte, P. (1992) *J. Biol. Chem. 267*, 6736–6742.
Yeung, A. T., Mattes, W. B., & Grossman, L. (1986) *Nucleic Acids Res. 14*, 2567–2582.
Yeung, A. T., Dinehart, W. J., & Jones, B. K. (1988) *Nucleic Acids Res. 16*, 4539–4554.